Journal of Materials Chemistry C

Accepted Manuscript

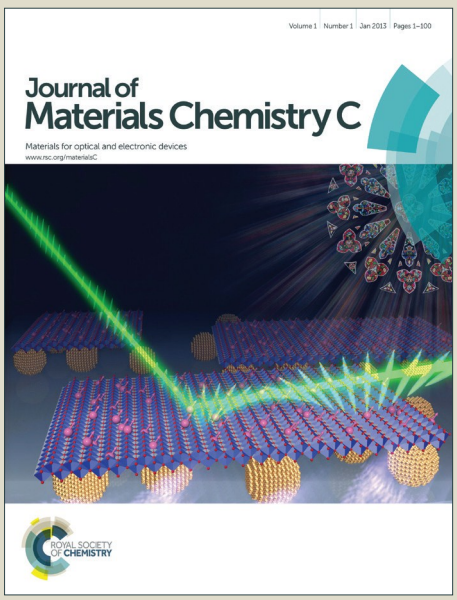

ROYAL SOCIETY OF CHEMISTRY

www.rsc.org/materialsC

Journal Name

ARTICLE

Delaminated Layered Rare-Earth Hydroxide Composites with Ortho-Coumaric Acid: Color-tunable luminescence and Blue Emission due to Energy Transfer

Received 00th January 20xx,
Accepted 00th January 20xx

DOI: 10.1039/x0xx00000x

www.rsc.org/

Feifei Su,[a] Qingyang Gu,[a] Shulan Ma,[a,*] Genban Sun,[a] Xiaojing Yang,[a] Li-Dong Zhao[b]

We demonstrate a novel example of delaminated layered rare-earth hydroxide (LRH, R= Tb, Y) composites with ortho-coumaric acid (*abbr.* CMA) and surfactant 1-octane sulfonic (*abbr.* OS) anions that exhibit tunable photoluminescence especially blue emission due to energy transfer *via* layer Tb^{3+}. Different molar ratios of organic guests (OS/CMA) and layer ions (Tb/Y) give rise to versatile composites of OS_xCMA_{1-x}-$LTb_yY_{1-y}H$ (x = 0.9, 0.8, 0.7, 0.6, 0.5, y = 1, 0.9, 0.7, 0.5, 0.3, 0.1, 0). In solid state, for LTbH composites, co-quenching for emissions of CMA and layer Tb^{3+} is found, while for LYH composites, green emission (502 nm) is observed. In formamide (FM), all of the composites are found to be facilely delaminated, and the colloidal suspensions of LTbH composites with varied OS_xCMA_{1-x} interlayer guests exhibit tuning-color within blue-light region (430-465 nm), with blue-shift of emissions and enhanced luminous intensity following increscent OS content. $LTb_yY_{1-y}H$ composites (with a fixed OS/CMA ratio of 0.7:0.3), however, present emissions from blue to green following increased Y^{3+} contents. A new concept of 'host-energy transfer-induced-emission (HETIE)' is proposed to explain the blue luminescence *via* energy transfer of host Tb^{3+}. The intriguing energy transfer between photoactive host matrix and interlayer guests in delaminated state offers a promising approach to achieve efficient tuning of luminescence, thus meeting the high demand of applications on multicolor optical and display devices especially blue emission.

Introduction

The fabrication of inorganic-organic hybrid phosphors with ordered structure and particular property has attracted increasing attention. Depending on the inorganic and organic components as well as their interactions, the formed composites generate a wide variety of properties. Two-dimensional (2D) layered materials[1] can serve as inorganic matrices to assemble hybrid materials with variable guests and tunable volume in interlayer. Moreover, the loading of photoactive guests and their arrangement within the 2D matrix can be regulated, which facilitates the modulation of luminescence.[2, 3] Layered double hydroxides (LDHs) are one type of the 2D matrices with positive-charged layers, whose adjustable interlayer compositions and space provide a large number of applications.[2, 4-9] The easier penetration of LDH interlayer channels has facilitated the realization of optical/chemical sensors with rapid response and recyclability.[2, 10, 11] Much progress has been made in the development of LDH-chromophore hybrids,[12-20] however, most of them focused on the luminescence property of the involved chromophores rather than the LDH hosts, because the LDH layer ions are generally not photoactive thus only serving as inorganic matrices. The synergetic effect of organic chromophores and 2D layers that hold photoactive ions such as Eu^{3+}, Tb^{3+} or Dy^{3+} has not been established to date.

Recently, layered rare earth hydroxides (LRHs), a newly emerging class of 2D hosts, have attracted increasing interest.[21-25] The LRHs have positively-charged layers similar to LDHs but the host layers contain lanthanide elements, whose particular nature provide the unique applications in ion exchange,[26] catalysis,[21] adsorption,[27] photoluminescence (PL),[28] and etc. It is expected LRH-chromophores can improve the photophysical and photochemical properties as well as photostability of the organic chromophores, sometimes may alter the luminescence feature arising from the synergetic effect. With regard to LRH/organic composites, most of the investigations focused on Eu-involving LRHs, for example our recent work for LEuH, LYH:Eu and LGdH:Eu, in which enhancement or quenching for Eu^{3+} luminescence by the introduced organics was found.[29-32] Studies on layered terbium hydroxide (LTbH) composites with organic compounds are relatively rare,[33, 34] and they mainly involve the luminescence of the layer Tb^{3+} rather than interlayer organics.

[a] *Beijing Key Laboratory of Energy Conversion and Storage Materials, College of Chemistry, Beijing Normal University, Beijing 100875, P. R. China. Fax: 86 10 5880 2075; Tel: 86 10 5880 7524; E-mail: mashulan@bnu.edu.cn.*
[b] *School of Materials Science and Engineering, Beihang University, Beijing, 100191, China.*

† Electronic Supplementary Information (ESI) available: excitation spectra of Cl-LTbH, CMA-Na and composites $OS_{0.9}CMA_{0.1}$-LTbH and $OS_{0.7}CMA_{0.3}$-$LTb_yY_{1-y}H$, emission spectra of Gd(III) complex of CMA (Gd-CMA) under 240 nm excitation at room temperature, phosphorescence spectrum of Gd-CMA in methanol solution (77 K), excitation spectra of CMA-Na and composites OS_xCMA_{1-x}-LTbH and $CMA_{0.7}OS_{0.3}$-$LTb_yY_{1-y}H$ in FM. See DOI: 10.1039/x0xx00000x

With regard to actural applications of luminescent materials, facile fabrication of ordered films is crucial, while most of the investigations focus on LDH nannosheets. This may result from the easier delamination of LDH system.[18, 19, 35-37] LRH nanosheets would be a new class of functional 2D building blocks[38-41] for assembly of ultrathin films, but the difficulty in delamination and low concentration of the delaminated LRH nanosheets restrict their applications. In our recent communication,[42] we found the co-intercalation of anion surfactant OS (1-octane sulfonic acid sodium salt) and fluorescent molecule 8-hydroxy-pyrene-1,3,6-trisulphonate (*abbr*. HPTS) into LEuH could achieve one-step delamination of the formed composites. This beneficial way may be extended to other LRH systems for fabrication of new kinds of luminous materials. We have recently intercalated two coumaric acids into LEuH/LGdH systems and found different intercalation structures and photoluminescence property,[43] but intensive study of the delamination on luminescence property and mechanism are lacking.

In this work, we select OS and ortho-coumaric acid (*abbr.* CMA, whose molecular structure can be referred to Scheme 1) as organic guests to co-intercalate into layered rare-earth hydroxide (LRH, R= Tb, Y) to study the structure and luminescence property. The CMA is one of the best phenolic acids that have biological activity inhibits intracellular triglyceride and glycerol-3-phosphate dehydrogenase activity.[44] Besides, CMA is a photoactive organic compound that would present luminescent property. We observe that in solid state, co-quenching for luminescence of Tb^{3+} and CMA, while in delaminated colloidal state in formamide (FM), the LTbH composites exhibited blue emissions, in sharp contrast to the green emission of LYH composites. Importantly, we found, for the first time, the varied OS/CMA ratios or Tb/Y ratios can regularly control the emission wavelengths and intensity, which showed efficient and excellent color-tuning behavior.

Experimental Section

Synthetic procedures

Preparation of Cl-LRH precursors.

Tb_4O_7 (99.9%) were obtained from Nonferrous Metal Research Institute Rare Earth New Materials Co., Ltd. 1-octanesulfonic acid sodium salt and hexamethylenetetramine (HMT) were purchased from Beijing HWRK Chemical Co., Ltd. and Xi Long Chemical Co., Ltd, respectively. The o-coumaric acid (CMA) was acquired by TCI (Shanghai) Development Co., Ltd. Formamide (FM) is from the Tianjin Bodi Chemical Co., Ltd. Methanol, HCl, NaOH and NaCl were obtained from Beijing Chemical Co., Ltd. The synthesis of $TbCl_3{\cdot}6H_2O$ were referenced the reported work.[39]

The Cl-LTbH was synthesized *via* a hydrothermal reaction of $TbCl_3{\cdot}6H_2O$ using hexamethylenetetramine (HMT) as the hydrolysis reagent.[45] An aqueous solution containing $TbCl_3{\cdot}6H_2O$ (1mmol), HMT (1 mmol), NaCl (13 mmol), and deionized water (80 mL) was heated at 90 °C for 12 h in a Teflon autoclave. The obtained products were filtered, washed with deionized water to remove impurities, and then vacuum dried at 40 °C for 24 h.

For Cl-$LTb_yY_{1-y}H$, the total amount of $TbCl_3{\cdot}6H_2O$ and $YCl_3{\cdot}6H_2O$ was 1 mmol, and the rest synthesis procedures was similar to Cl-LTbH. Taking Cl-$LTb_{0.9}Y_{0.1}H$ as an example, the aqueous solution containing $TbCl_3{\cdot}6H_2O$ (0.9 mmol, 0.336 g) and $YCl_3{\cdot}6H_2O$ (0.1 mmol, 0.030 g), HMT (1 mmol), NaCl (13 mmol), and deionized water (80 mL) was heated at 90 °C for 12 h in a Teflon autoclave. The obtained samples were filtered, washed with deionized water to remove impurities, and then vacuum dried at 40 °C for 24 h.

Intercalation of OS/CMA guests into LRH by ion exchange.

The co-intercalations of OS_x/CMA_{1-x} anions into $LTb_yY_{1-y}H$ were carried out through ion-exchange under hydrothermal condition. Firstly, CMA was deprotonated beforehand by adding 1:1 stoichiometric NaOH to generate corresponding anion solutions (~80 mL), followed by mixed with OS. For all of the composites, the total amount of OS and CMA is 3 mmol, with only varying the molar rations of OS_x/CMA_{1-x} as x = 1.0, 0.9, 0.8, 0.7, 0.6, and 0.5. For $OS_{0.9}CMA_{0.1}$-LTbH, 0.3 mmol (0.012 g) NaOH and 0.3 mmol (0.049 g) CMA were dissolved in 80 mL deionized water, then 2.7 mmol (0.584 g) OS was added to the above solution. Then 0.43 mmol (~0.1 g) Cl-$LTb_yY_{1-y}H$ powder was dispersed into the above solution. The reactions were conducted at 70 °C for 24 h in Teflon-autoclaves. The resulting precipitates were collected by filtration, washed with deionized water, and vacuum dried at 40 °C for 24 h.

Synthesis of Gd(III) complex of CMA (CMA-Gd).

Firstly, 0.6 mmol (0.270 g) $Gd(NO_3)_3{\cdot}6H_2O$ was dissolved in 3 mL H_2O, then the solution was mixed with 5 mL methanol containing 0.6 mmol (0.098 g) CMA. The pH value of mixed solution was adjusted to ~6.8 using dilute NaOH solution. The as-obtained solution was evaporated by heating until the rest of the solution is about 1 mL. After cooled, the Gd-CMA complex was precipitated out, and vacuum dried at 40 °C for 24 h.

Delamination of the as-prepared composites in FM.

0.05 g composites or CMA-Na was put into 20 mL FM by mechanical shaking for 12 h, to form translucent colloid suspensions or a solution for CMA-Na. The composites were found to be delaminated in FM.

Characterization Techniques.

The powder X-ray diffraction(XRD) patterns were collected by using a Phillips X'pert Pro MPD diffractometer with Cu-*K*α radiation at room temperature, with a step size of 0.0167°, a scan time of 15 sper step, and a 2ϑ value ranging from 4.5 to 70°. The generator settings were 40 kV and 40 mA. For the small degrees, the XRD patterns were measured at room temperature with step size of 0.008 °, scan time of 30 seconds per step. Fourier transformed infrared (FT–IR) spectra of the samples were recorded with a Nicolet 380 Fourier transform infrared spectrometer by the KBr method. Scanning electron microscope (SEM), elemental distribution mapping, and energy dispersive spectroscopy (EDS) measurements were carried out using a Hitachi S-4800 microscope. Luminescence spectra were measured at room temperature with RF-5301PC spectrofluorimeter and Cary Eclipse spectrofluorimeter. 0.15 g sample was tabletting by tablet machine under 20 KPa in room temperture, then testing the solid luminescence. The phosphorescence spectra of samples were measured at 77 K in a methanol solution on a Hitachi F-7000 FL Spectrophotometer.

The metal ion contents were determined by inductively coupled plasma (ICP) atomic emission spectroscopy (Jarrel-ASH, ICAP-9000) after the solid products were dissolved in a 0.1 m HCl solution. C, H, and N contents were determined by using an Elementar vario EL elemental analyzer. The chemical formulas of the products were calculated from the results of ICP and CHN analyses.

Results and Discussion

Structures and compositions of Cl-LRH precursors and composites. The XRD patterns of Cl-LTbH precursor, composites of OS-LTbH and OS_xCMA_{1-x}-LTbH were displayed in Fig. 1A. The Cl-LTbH (Fig. 1A-a) has a basal spacing (d_{basal}) of 0.83 nm, showing a series of (*00l*) reflections being characteristic of a layered rare-earth hydroxide.[45] The sharp and symmetric diffractions suggest the high crystallinity of Cl-LTbH. After ion-exchange of Cl-LTbH with different proportions of OS/CMA anions, the resulting products revealed enlarged d_{basal} values of 1.97-2.15 nm (Fig. 1A-b-g). The OS_xCMA_{1-x}-LTbH (x > 0.6) with high OS contents (Fig. 1A-b-e) had similar XRD patterns meaning single phases. For $OS_{0.8}CMA_{0.2}$-LTbH, as an example, a series of diffraction peaks (Fig. 1A-d,d') at 1.98, 1.00, 0.67, 0.50 and 0.40 nm were observed, demonstrating a d_{basal} of 1.98 nm. The difference of characteristic peaks in LRH composites and Cl-LTbH precursor results from the substitution of the OS and CMA anions for Cl^- in the interlayer of LTbH. The much larger size of OS and CMA than that of Cl^- leads to the larger interlaminar spacings. For the OS_xCMA_{1-x}-LRH composites themselves, the difference of characteristic peaks come from the different size of OS and CMA anions and their varied relative contents. Based on the thickness of LRH layer of 0.65 nm[29] and the height of 0.82 nm for CMA (dimension is ~0.82×0.46×0.31 nm) and 1.04 nm for OS (1.04×0.37×0.26 nm), the gallery spacing for these composites of ~1.33 nm (=1.98-0.65) corresponded to an alternating bi-layered arrangement for CMA with adjacent monolayer OS (Scheme 1c). The composites with high CMA contents (smaller *x* values), taking $OS_{0.6}CMA_{0.4}$-LTbH and $OS_{0.5}CMA_{0.5}$-LTbH (Fig. 1A-f,g) as samples, revealed similar splitting peaks, showing two sets of diffraction peaks and two bigger d_{basal} of 2.15 and 2.09 nm, respectively. This demonstrates that CMA anions dominantly supported the interlayer due to their high amount (Scheme 1b). As discussed below, the presence of the two separated phases of OS-LTbH and CMA-LTbH did not affect their delamination results. The 0.31 nm peak, originating from the non-basal (220) reflection representing the feature of the LRH host layer,[46] retained in all of the composites. The CMA anion arising from one deprotonated $-COO^-$ group preferred to the bi-layered alternating antiparallel arrangement (Scheme 1b,c), for which the negatively-charged $-COO^-$ groups combined with the positively-charged LRH layers *via* electrostatic interactions, and also, the π-π stacking interactions between benzene rings further assured the stable structure.

For the $OS_{0.7}CMA_{0.3}$-$LTb_yY_{1-y}H$ composites with a fixed OS/CMA molar ratio of 0.7:0.3, the XRD patterns (Fig. 1B) are much similar, except the increscent d_{basal} values following the increased Y content (decreased *y* value). As known, the Y^{3+} has a smaller ion radius (0.089 nm) than that of Tb^{3+} (0.092 nm), but the composites with increased Y^{3+} amount in layers showed bigger d_{basal} values, which may be owing to the high hydration ability of Y^{3+} than the lower hydrated Tb^{3+}.[8] At the OS:CMA molar ratio of 0.7:0.3, all of the formed composites with different doped layers are almost with single phases, also suggesting the Y^{3+} and Tb^{3+} were located in the same layer.

Through ICP and CHN analyses and charge balance consideration, the compositions for the LRH precursors and composites were determined and some of them were listed in Table 1. We can see from Table 1 that the charge of CMA is -1 valence, coincident with the starting NaOH/CMA molar ratio of 1:1 to make CMA deprotonated. All of the composites had accordant molar ratios for OS/CMA and Tb/Y with those added in the starting materials. The small errors of calculated elemental contents compared with experimental values show the estimated chemical formulas are reasonable.

IR data and morphologies of Cl-LRH precursor and composites.

The FT-IR spectra of the as-prepared precursors and the composites were shown in Fig. 2. For CMA (Fig. 2a), the bands at 1669 and 1461 cm^{-1} corresponded to the stretching of the C=O and C-OH bonds. For OS (Fig. 2b), the bands at 1200 and 1065 cm^{-1} were assigned to SO_3^- absorption,[35, 47] and those at 2920 and 2851 cm^{-1} were ascribed to ν_{as} and ν_s stretching vibrations of aliphatic $-CH_2$ and $-CH_3$ groups, respectively. After intercalation, the bands at 2921 and 2853 cm^{-1} ascribed to -C-H vibrations clearly signified the introduction of OS into the interlayer (Fig. 2c,d). The vibrations of SO_3^- group appeared at 1171 and 1049 cm^{-1}. The ν_{as} and ν_s stretching vibrations of $-COO^-$ were observed at 1533 and 1412 cm^{-1}, for which the bathochromic shift due to the deprotonation. The peak related to M-O stretching/bending vibrations[22] at 637 cm^{-1} in Cl-LTbH precursor (Fig. 2a) shifted to 606 cm^{-1} in the composites and a new band at 430 cm^{-1} appeared (Fig. 2c,d), indicating the interactions of the introduced guests with the layer hydroxides.

Fig. 3 showed SEM images of the as-prepared samples. Cl–LTbH precursor (Fig. 3a,a') was crystallized into regular hexahedron platelets and grew into columnar or flower-like aggregates.[34] The hexahedron platelets of Cl-LTbH are similar to that of the LDyH compounds,[8] which are consistent with that Geng et al. reported,[23] possibly due to the close radius of Tb^{3+} to Dy^{3+} and their similar crystal cell. Compared with LGdH[27] and LEuH,[31] the Cl-LTbH had shorter broadside. The composites (Figs. 3b-l) remained the morphology of the precursors, implying a topotactic intercalation of the interlayer species.[7, 9]

Fig. 4 displayed the EDS and elemental mappings of Tb, Y, and S in $CMA_{0.7}OS_{0.3}$-$LTb_yY_{1-y}H$ (a, b, c, corresponding to y=0.7, y=0.5, y=0.3, respectively) samples. The relative molar ratios of the three samples obtained by EDS are consistent with those added in the starting materials, which indicates a nearly complete reaction of the cations in the LTb/YH layers. The relative brightness of each element represents the content corresponding to its composition in the sample. The three elements exhibited an unanimous distribution of density following the thickness of the LRH plates.

Luminescence property of samples in solid state.

As shown in Fig. 5A-a, the powdered Cl-LTbH (measured with the excitation wavelength of 352 nm of Tb^{3+}) depicted characteristic Tb^{3+} emission peaks at 485, 545, 586 and 619 nm, respectively assigned to $^5D_4$–^7F_J (*J* = 6, 5, 4, 3) radiative-relaxational transitions of

Tb^{3+}.[48] The CMA sodium salt (CMA-Na) in solid state, showed cyan luminescence with the maximum emission of 480 nm (Fig. 5A-b). In the composite $OS_{0.9}CMA_{0.1}$-LTbH, however, neither emission of layer Tb^{3+} nor emission of CMA-Na was observable (Fig. 5A-c), no matter which of the excitation wavelengths of 352 nm for Tb^{3+} or 420 nm for CMA-Na (excitation spectra was shown in Fig. S1†) was used. The composites with Y-doped layers of $LTb_yY_{1-y}H$ (Figs. 5B-b,c,d), in contrast, revealed distinct green emission at 502 nm. Following the increscent Tb^{3+} amount, the position of this peak was invariant while the emission intensity was weakened, demonstrating the influence of Tb^{3+}. The enhanced emission intensity and changed emission position for CMA-Na within LYH layers (Fig. 5B) indicate the host layers play an important role for preventing the inter-molecular aggregation of CMA-Na arising from π-π interactions etc. [49]

The co-quenching for emissions of CMA and layer Tb^{3+} may be ascribed to an energy transfer between the layer Tb^{3+} and interlayer CMA anions. The excitation wavelengths for Tb^{3+} are 300-390 nm (Fig. S1A-a†), and excitation wavelengths for CMA-Na salt are 350-500 nm (Fig. S1A-b†), from which we can see the needed energy for Tb^{3+} excitation is lower than that for CMA, so the provided energy would be absorbed preferentially by Tb^{3+}. Whereas, there is certain overlap for the excitation range for CMA (350-500 nm, Fig. S1A-b†) and emission for Tb^{3+} (450-650 nm, Fig. 5A-a), and also the emissions of CMA (300-650 nm emissions at 240 nm excitation, here is for CMA-Gd complex, see Fig. S2†) and excitations for Tb^{3+} (300-400 nm, Fig. 5A-a) also had some overlaps, which mean that there would be mutual energy transfer between Tb^{3+} and CMA, thus possibly causing the co-quenching effect. Meanwhile, the high-energy vibration of -OH of CMA anions would also compete the porvided energy to generate nonradiative relaxation channels,[42] which accelerated the co-quenching effect. Similar co-quenching phenomenon was found in our previous work for LEuH-HPTS composites.[42]

Luminescence of OS_xCMA_{1-x}-LTbH composites at delaminated state in FM.

When the composites dispersed in FM for only 30 min, transparent colloidal suspensions were found to be formed, revealing obvious Tyndall lights cattering (Fig. 6a) suggesting the delamination. For LRH system, the delamination is rather difficult and delamination degree is generally low.[38, 39, 41] In our recent communication,[42] we found adding surfactant OS for intercalation into LRH can realize facile one-step delamination of the formed composites. Now the present results further verified the delamination. The as-obtained transparent colloidal suspensions assured the convenient luminescence measurement and characterization, especially subsequent fabrication of films based on delaminated LRHs. If without addition of OS, the as-prepared composites cannot be completely delaminated though under much long time (3 days or long) when dispersed in FM.

Fig. 7A showed the emission spectra of CMA-Na and LTbH-involving composites (OS_xCMA_{1-x}-LTbH) dispersed in FM. Free CMA anions in FM solution exhibited a peak at 502 nm (Fig. 7A-a) belonging to green luminescence. This green emission for CMA-Na in solution is different from that observed in its solid state (cyan emission at 480 nm), but the same as found for the LYH compsoites (502 nm, for OS_xCMA_{1-x}-LYH) in solid state discussed above. The LTbH composites, in a sharp contrast to free CMA, revealed distinct blue luminescence, and the emission wavelengths shifted from 465 nm to 430 nm following the increased OS content (*x* value), as shown in Fig. 7A-b-f. Moerover, enhanced emission intensity with the increase of OS content was observable, indicating the significant function of the surfactant OS. The x/y emission color coordinates depicted in the 1931 CIE chromaticity diagram (Fig. 7A') demonstrated that the color of the composites could be tuned by varying the composition ratios of OS/CMA incorporated with LTbH layers, achieving the controllable emissions within blue-light region. The blue shift phenomenon was also observed in hydrothermally treated DDS–AQS/LDH.[17]

Ogawa and Kuroda reported surfactants can alter the aggregation of photoactive species.[50] The surfactant (here is OS) would dilute/isolate CMA anions so as to prevent their aggregation that weakens the luminescence.[49, 51, 52] The co-intercalation of hybrids into layered matrices would be possibly not only for the maximization of luminescence efficiency but to save manufacturing cost.[17] In present system, the OS serving as an anionic sufactant affected the emission intensity as well as the peak position, in contrast to that Ramon reported.[53] The change of the emission position may be owing to a microenvironment change of the CMA anions when different amounts of OS intercated with CMA and the positive-charged LRH layers. Some supramolecular structures *via* intermolecular interactions between rigid CMA and flexible OS anions may also be formed thus leading to the change of the configuration of CMA as reported in other compunds,[54, 55] so as to alter the energy levels of CMA then the luminescence behaviors. Therefore, *via* altering the relative amounts of photoactive CMA and surfactant OS interacted with LTbH layers, color-tuning within the favorite blue-light region was achieved.

Luminescence of composites with doped layers Y:LTbH at delaminated state in FM.

Fig. 7B displayed the emission spectra of the composites for doped $LTb_yY_{1-y}H$ layers dispersed in FM. Here we used a fixed molar ratio of OS/CMA of 0.7:0.3 and only changed the molar ratios of layer Tb/Y ions as 1:0, 0.9:0.1, 0.7:0.3, 0.5:0.5, 0.3:0.7 and 0.1:0.9 and 0:1. The composites were labled as $OS_{0.7}CMA_{0.3}$-$LTb_yY_{1-y}H$. Following the increased Y^{3+} content (decreased y value), regularly change of emission wavelegths from blue (450 nm) to green (500 nm) was found. Using the colloidal suspensions of $CMA_{0.7}OS_{0.3}$-$LTb_{0.9}Y_{0.1}H$ and $CMA_{0.7}OS_{0.3}$-LYH, we wrote the characters of 'ABC' on paper, which revealed the bright blue and green color (Fig. 6b,c). Aditionally, the composites with host layers containing more Y^{3+} exhibited increased luminescence intensity, which shows the Y^{3+} in the layers played a very important role in helping the host absorb energy, as Gd^{3+} did in other work.[33] This highlights the important function of the host layer ions on the adjustment of fluorescence color. The emission color coordinates in the 1931 CIE chromaticity diagram shown in Fig. 7B' depicted the color crossing from blue to green region for the corresponding composites.

The different excitation wavelengths (Fig. S4†) of the LYH-involving composites and LTbH-involving composites also demonstrated the varied energy absorption species in the two cases. For LYH system, the excitation originated mainly from the

CMA anions (375 nm, Fig. S4B†), while in the LTbH composites, the excitation or energy absorption is mainly *via* Tb^{3+} (~355 nm excitation, Fig. S4A†) rather than that *via* CMA. The different absorption centers account for the various luminescence behaviors.

Energy level analysis and energy-transfer mechanism.

As shown in Scheme 2, we can see in contrast to the co-quenching in solid state for LTbH composites (Scheme 2A), the delaminated LTbH composites in FM contributed to blue luminescence (Scheme 2B), meanwhile, the LYH layers advanced green luminescence reflecting emission of CMA (Scheme 2C). The blue luminescence of LTbH system may arise from an energy transfer and synergetic effect between layer Tb^{3+} and CMA anions. Note that when more than one kind of phosphors were present in proximity to each other, only the emission from that with the lower excited state energy would be observed.[56] The triplet energy level of CMA was determined by using the low-temperature phosphorescence spectra of the Gd-CMA complex.[57] The complex exhibited CMA phosphorescence as a band centered at 634 nm under excitation at 240 nm at 77 K in a methanol solution (Fig. S3†). The triplet energy level (T1) of CMA was estimated by referring to the shortest wavelength emission edge (625 nm, ~16000 cm^{-1}) in the spectrum. The triplet energy level of ~16000 cm^{-1} for CMA was lower than that of the $^5D_4$ levels of Tb^{3+} (20545 cm^{-1}),[58] demonstrating the emission of CMA would be preferentially observed. In this case, the host Tb^{3+} would primarily absorb the energy and then transfer it to CMA for emission. This is consistent with the excitation spectra in LTbH composites, in which the energy absorption was mainly by Tb^{3+} rather than by CMA (Fig. S4A†).

Consequently, for LTbH composites, the Tb^{3+}-containing host layers acted not only as host matrices for the photoactive CMA anions, but also served as energy-transfer bridges that connect the host layers and CMA to intensify or alter the emission of CMA by a cascaded energy transfer, similar to those reported.[56, 59, 60] We propose that the blue emission for Tb^{3+}-containing composites was mainly caused by a 'host(Tb^{3+})-energy transfer-induced-emission' (*abbr*. 'HETIE') process. Generally, in the cases that host layers include photoactive lanthanides such as Eu^{3+}, Tb^{3+} or Dy^{3+}, and the interlayer has chromophores, when their emission and excitation regions were overlapped, an energy transfer may exist, which led to co-quenching or fantastic luminescence behaviours. Here in delaminated state in FM, the host sheets are highly free and could combine tightly with the CMA anions *via* electrostatic interactions, being much different from the interactions in solid state, thus producing the disparate emission results.

On the basis of all of the above results, the energy-transfer pathway for the CMA luminescence involved the following steps (Scheme 3): (i) For LYH-CMA system, *via* Y^{3+}-induced increased absorption cross-section as Gd^{3+} usually did,[33] the LYH hosts helped absorb the energy, then followed by an energy transfer to CMA; (ii) For LTbH:Y-CMA system, UV absorption initially performed by the LYH host layers, followed by layer Tb^{3+} ions acting as energy-transfer bridges that connect the host and CMA, to achieve the emission of CMA; (iii) For LTbH-CMA system, the host Tb^{3+} ions preferentially absorbed the energy and then transferred it to CMA, in which the energy transfer or intersystem crossing probably contributed to the blue emission. Furthermore, under delaminated state in polar solvents, the microenvironment of CMA encapsulated by LTbH sheets could be altered significantly, thus probably causing the change of the triplet energy levels, which resulted in the favourite emissions.

Conclusions

In summary, co-intercalations of photoactive ortho-coumaric acid (*abbr.* CMA) and surfactant 1-octane sulfonic anions (*abbr.* OS) into LRH (R= Tb, Y) gave rise to composites OS_xCMA_{1-x}-$LTb_yY_{1-y}H$ exhibiting tunable fluorescence especially blue emission. In solid state, LYH layers facilitated the green emission of CMA, while LTbH layers led to a co-quenching effect due to energy transfer between the interlayer CMA and layer Tb^{3+}. In FM, all of the composites were found to be facilely delaminated, and the as-formed colloidal suspensions of composites exhibited versatile luminescence. For LTbH layers, through changing the relative amounts of CMA/OS guests, controllable emissions in blue-light region (430-465 nm) can be achieved. For Y^{3+} doped layers ($LTb_yY_{1-y}H$), however, emissions from blue to green were obtained with the increscent Y content. The excitaion wavelegths and energy levels were used to explain the energy transfer. The overlaps of emissions and excitaion regions would lead to the synergetic energy transfer thus resulting in the co-quenching or favorite luminecscence behaviors. The delaminated positively-charged LTbH nanosheets with high freedom can combine tightly with the negatively-charged CMA anions, thus varying the microenvironment and thus the triplet energy levels of CMA anions so favoring the blue emissions. A concept of 'host-energy transfer-induced-emission' ('HETIE') was issued for accounting for the synergetic energy transfer during the new kind of LRH/chromophores. The facile delamination of composites and the effective energy-transfer can be expanded to more other hybrid systems involving photoactive host layer ions and interlayer species, which offers a new and beneficial way to fabricate multi-color luminous materials especially the favorite blue emissions, or other desirable or fantastic luminescence.

Acknowledgments.

This work is supported by the National Science Foundations of China (21271028, 51272030 and 21271001).

1. T. J. Tambach, P. G. Bolhuis and B. Smit, *Angew. Chem. Int. Edit.*, 2004, **43**, 2650.
2. D. P. Yan, J. Lu, J. Ma, M. Wei, D. G. Evans and X. Duan, *Angew. Chem. Int. Ed.*, 2011, **50**, 720.
3. C. Seebacher, J. Rau, F. W. Deeg, C. Brauchle, S. Altmaier, R. Jager and P. Behrens, *Adv. Mater.*, 2001, **13**, 1374.
4. S. L. Ma, L. Huang, L. J. Ma, Y. Shim, S. M. Islam, P. Wang, L.-D. Zhao, S. C. Wang, G. B. Sun, X. J. Yang, M. G. Kanatzidis, *J. Am. Chem. Soc.*, 2015, **137**, 3670.
5. S. L. Ma, C. H. Fan, L. Du, G. L. Huang, X. J. Yang, W. P. Tang, Y. Makita and K. Ooi, *Chem. Mater.*, 2009, **21**, 3602.
6. X. Y. Xue, Q. Y. Gu, G. H. Pan, J. Liang, G. L. Huang, G. B. Sun, S. L. Ma and X. J. Yang, *Inorg. Chem.*, 2014, **53**, 1521.

7. S. L. Ma, Y. Shim, S. M. Islam, K. S. Subrahmanyam, P. L. Wang, H. Li, S. C. Wang, X. J. Yang and M. G. Kanatzidis, *Chem. Mater.*, 2014, **26**, 5004.
8. J. B. Liang, R. Z. Ma and T. Sasaki, *Dalton. Trans.*, 2014, **43**, 10355.
9. S. L. Ma, S. M. Islam, Y. Shim, Q. Y. Gu, P. L. Wang, H. Li, G. B. Sun, X. J. Yang and M. G. Kanatzidis, *Chem. Mater.*, 2014, **26**, 7114.
10. D. P. Yan, J. Lu, M. Wei, J. B. Han, J. Ma, F. Li, D. G. Evans and X. Duan, *Angew. Chem. Int. Edit.*, 2009, **48**, 3073.
11. Z. Li, J. Lu, S. D. Li, S. H. Qin and Y. M. Qin, *Adv. Mater.*, 2012, **24**, 6053.
12. B. Johann, B. Peter, S. Markus and L. Heinz, *Adv. Funct. Mater.*, 2003, **13**, 241.
13. D. P. Yan, J. Lu, M. Wei, S. Qin, L. Chen, S. Zhang, D. G. Evans and X. Duan, *Adv. Funct. Mater.* , 2011, **21**, 2497.
14. D. P. Yan, J. Lu, J. Ma, S. Qin, M. Wei, D. G. Evans and X. Duan, *Angew. Chem. Int. Ed.*, 2011, **50**, 7037.
15. Z.-L. Wang, Z.-H. Kang, E.-B. Wang, Z. M. Su and L. Xu, *Inorg. Chem.*, 2006, **45**, 4364.
16. S. L. Dang, D. P. Yan and J. Lu, *J. Solid. State. Chem.*, 2012, **185**, 219.
17. S. Li, J. Lu, M. Wei, D. G. Evans and X. Duan, *Adv. Funct. Mater.*, 2010, **20**, 2848.
18. W. J. Guan, J. Lu, W. J. Zhou and C. Lu, *Chem. Commun.*, 2014, **50**, 11895.
19. Y. M. Qin, J. Lu, S. D. Li, Z. Li and S. F. Zheng, *J. Phys.Chem. C*, 2014, **118**, 20538.
20. D. P. Yan, J. Lu, M. Wei, D. G. Evans and X. Duan, *J. Phys. Chem. B*, 2009, **113**, 1381.
21. F. Gandara, J. Perles, N. Snejko, M. Iglesias, B. Gomez-Lor, E. Gutierrez-Puebla and M. A. Monge, *Angew. Chem.*, 2006, **45**, 7998.
22. F. X. Geng, H. Xin, Y. Matsushita, R. Ma, M. Tanaka, F. Izumi, N. Iyi and T. Sasaki, *Chem. Eur. J.*, 2008, **14**, 9255.
23. F. X. Geng, Y. Matsushita, R. Z. Ma, H. Xin, M. Tanaka, N. Iyi and T. Sasaki, *Inorg. Chem.*, 2009, **48**, 6724.
24. J. B. Liang, R. Z. Ma, F. X. Geng, Y. Ebina and T. Sasaki, *Chem. Mater.*, 2010, **22**, 6001.
25. F. X. Geng, R. Z. Ma and T. Sasaki, *Acc. Chem. Res.*, 2010, **43**, 1177.
26. K. H. Lee and S. H. Byeon, *Eur. J. Inorg. Chem.*, 2009, 929.
27. W. L. Li, Q. Y. Gu, F. F. Su, Y. H. Sun, G. B. Sun, S. L. Ma and X. J. Yang, *Inorg. Chem.*, 2013, **52**, 14010.
28. Q. Zhu, J. G. Li, C. Zhi, R. Ma, T. Sasaki, J. X. Xu, C. H. Liu, X. D. Li, X. D. Sun and Y. Sakka, *J. Mater. Chem.*, 2011, **21**, 6903.
29. N. K. Chu, Y. H. Sun, Y. S. Zhao, X. X. Li, G. B. Sun, S. L. Ma and X. J. Yang, *Dalton. Trans.*, 2012, **41**, 7409.
30. Q. Y. Gu, N. K. Chu, G. H. Pan, G. B. Sun, S. L. Ma and X. J. Yang, *Eur. J. Inorg. Chem.*, 2014, **3**, 559.
31. Q. Y. Gu, Y. H. Sun, N. K. i. Chu, S. L. Ma, Z. Q. Jia and X. J. Yang, *Eur. J. Inorg. Chem.*, 2012, **2012**, 4407.
32. Y. Sun, G. Pan, Q. Gu, X. Li, G. Sun, S. Ma and X. Yang, *Mater. Res. Bull.*, 2013, **48**, 4460.
33. L. L. Liu, Q. Wang, C. J. Gao, H. Chen, W. S. Liu and Y. Tang, *J. Phys. Chem. C*, 2014, **118**, 14511.
34. Y. S. Zhao, X. Y. Wang, M. J. Lu, Y. Yu, M. X. Guo and X. J. Yang, *Chinese. J. Inorg. Chem.*, 2014, **30**, 220.
35. S. Ida, D. Shiga, M. Koinuma and Y. Matsumoto, *J. Am. Chem. Soc.*, 2008, **130**, 14038.
36. V. V. Naik and S. Vasudevan, *Langmuir*, 2011, **27**, 13276.
37. W. Y. Shi, Y. K. Jia, S. M. Xu, Z. X. Li, Y. Fu, M. Wei and S. X. Shi, *Langmuir*, 2014, **30**, 12916.
38. L. F. Hu, R. Z. Ma, T. C. Ozawa and T. Sasaki, *Chem. Asian. J.*, 2010, **5**, 248.
39. Y. S. Zhao, J. G. Li, M. X. Guo and X. J. Yang, *J. Mater. Chem. C*, 2013, **1**, 3584.
40. Y. S. Yoon, B. I. Lee, K. S. Lee, G. H. Im, S. H. Byeon, J. H. Lee and I. S. Lee, *Adv. Funct. Mater.*, 2009, **19**, 3375.
41. K. H. Lee, B. I. Lee, J. H. You and S. H. Byeon, *Chem. Commun.*, 2010, **46**, 1461.
42. Q. Y. Gu, F. F. Su, S. L. Ma, G. B. Sun and X. J. Yang, *Chem. Commun.*, 2015, **51**, 2514.
43. Q. Y. Gu, F. F. Su, L. J. Ma, S. L. Ma, G. B. Sun and X. J. Yang, *J. Mater. Chem. C*, 2015, **3**, 4752.
44. C.-L. Hsu and G. C. Yen, *J. Agr. Food. Chem.*, 2007, **55**, 8404.
45. F. Geng, Y. Matsushita, R. Ma, H. Xin, M. Tanaka, F. Izumi, N. Iyi and T. Sasaki, *J. Am. Chem. Soc.*, 2008, **130**, 16344.
46. L. Wang, D. P. Yan, S. H. Qin, S. D. Li, J. Lu, D. G. Evans and X. Duan, *Dalton. Trans.*, 2011, **40**, 11781.
47. S. Sasaki, S. Aisawa, H. Hirahara, A. Sasaki, H. Nakayama and E. Narita, *J. Solid. State. Chem.*, 2006, **179**, 1129.
48. L. F. Hu, R.Ma, T. C. Ozawa and T. Sasaki, *Inorg. Chem.*, 2010, **49**, 2960.
49. J. Dong, K. M. Solntsev and L. M. Tolbert, *J. Am. Chem. Soc.*, 2009, **131**, 662.
50. M. Ogawa and K. Kuroda, *Chem. Rev.*, 1995, **95**, 399.
51. M. D. Curtis, J. Cao and J. W. Kampf, *J. Am. Chem. Soc.*, 2004, **126**, 4318.
52. M. S. Kwon, J. Gierschner, S. J. Yoon and S. Y. Park, *Adv. Mater.*, 2012, **24**, 5487.
53. B. R. Ramon and E. Joan, *J. Phys. Chem. B*, 2009, **113**, 1972.
54. J. B. Zhang, B. Xu, J. L. Chen, S. Q. Ma, Y. J. Dong, L. J. Wang, B. Li, L. Ye and W. J. Tian, *Adv. Mater.*, 2014, **26**, 739.
55. A. D. Shao, Z. Q. Guo, S. J. Zhu, S. Q. Zhu, P. Shi, H. Tian and W. H. Zhu, *Chem. Sci.*, 2014, **5**, 1383.
56. J. Ryu, S. Y. Lim and C. B. Park, *Adv Mater*, 2009, **21**, 1577.
57. M. Latva, H. Takalo, V. M. Mukkala, C. Matachescu, J. C. RodriguezUbis and J. Kankare, *J. Lumin.*, 1997, **75**, 149.
58. X. J. Zhou, X. Q. Zhao, Y. J. Wang, B. Wu, J. Shen, L. Li and Q. X. Li, *Inorg. Chem.*, 2014, **53**, 12275.
59. Y. C. Jia, W. Lu, N. Guo, W. Z. Lu, Q. Zhao and H. P. You, *Chem. Commun.*, 2013, **49**, 2664.
60. A. Balamurugan, V. Kumar and M. Jayakannan, *Chem. Commun.*, 2014, **50**, 842.

Journal Name

ARTICLE

Table 1. Chemical compositions for partial LRH precursors and OS_xCMA_{1-x}-LTb_yY_{1-y} H composites.

Samples	Chemical formula	Wt %, Found [Cal.]			
		Tb	Y	C	H
Cl-LTbH	$Tb(OH)_{2.52}(CO_3)_{0.07}Cl_{0.34}\cdot 0.8H_2O$	68.06 [68.31]	- -	0.37 [0.37]	1.78 [1.78]
Cl-$LTb_{0.9}Y_{0.1}$H	$Tb_{0.9}Y_{0.1}(OH)_{2.52}(CO_3)_{0.11}Cl_{0.26}\cdot 1.1H_2O$	62.35 [62.78]	3.84 [3.87]	0.58 [0.58]	1.87 [2.04]
Cl-$LTb_{0.3}Y_{0.7}$H	$Tb_{0.31}Y_{0.69}(OH)_{2.52}(CO_3)_{0.09}Cl_{0.31}\cdot 1.0H_2O$	26.22 [26.58]	32.34 [32.77]	0.55 [0.56]	2.23 [2.44]
Cl-$LTb_{0.1}Y_{0.9}$H	$Tb_{0.12}Y_{0.88}(OH)_{2.52}(CO_3)_{0.05}Cl_{0.39}\cdot 0.6H_2O$	12.04 [11.90]	47.22 [46.70]	0.37 [0.37]	2.40 [2.21]
Cl-LYH	$Y(OH)_{2.52}(CO_3)_{0.07}Cl_{0.33}\cdot 0.4H_2O$	- -	58.00 [57.68]	0.58 [0.58]	2.50 [2.16]
$CMA_{0.4}OS_{0.6}$-LTbH	$Tb(OH)_{2.41}(C_9H_7O_3)_{0.22}(C_8H_{17}O_3S)_{0.37}\cdot 2.5H_2O$	44.7 [45.04]	- -	16.68 [16.81]	4.00 [4.34]
$CMA_{0.3}OS_{0.7}$-$LTb_{0.9}Y_{0.1}$H	$Tb_{0.9}Y_{0.1}(OH)_{2.41}(C_9H_7O_3)_{0.19}(C_8H_{17}O_3S)_{0.40}\cdot 1.6H_2O$	42.52 [43,27]	2.64 [2.68]	17.56 [17.87]	4.14 [4.18]
$CMA_{0.3}OS_{0.7}$-$LTb_{0.3}Y_{0.7}$H	$Tb_{0.32}Y_{0.68}(OH)_{2.33}(C_9H_7O_3)_{0.20}(C_8H_{17}O_3S)_{0.47}\cdot 2.6H_2O$	14.91 [15.69]	18.06 [19.00]	19.83 [20.86]	4.76 [5.25]
$CMA_{0.3}OS_{0.7}$-$LTb_{0.1}Y_{0.9}$H	$Tb_{0.11}Y_{0.89}(OH)_{2.39}(C_9H_7O_3)_{0.19}(C_8H_{17}O_3S)_{0.42}\cdot 2.3H_2O$	5.93 [6.13]	26.27 [27.13]	20.42 [21.09]	5.03 [5.30]
$CMA_{0.3}OS_{0.7}$-LYH	$Y(OH)_{2.49}(C_9H_7O_3)_{0.16}(C_8H_{17}O_3S)_{0.35}\cdot 0.9H_2O$	- -	36.49 [36.93]	20.89 [21.15]	5.20 [4.70]

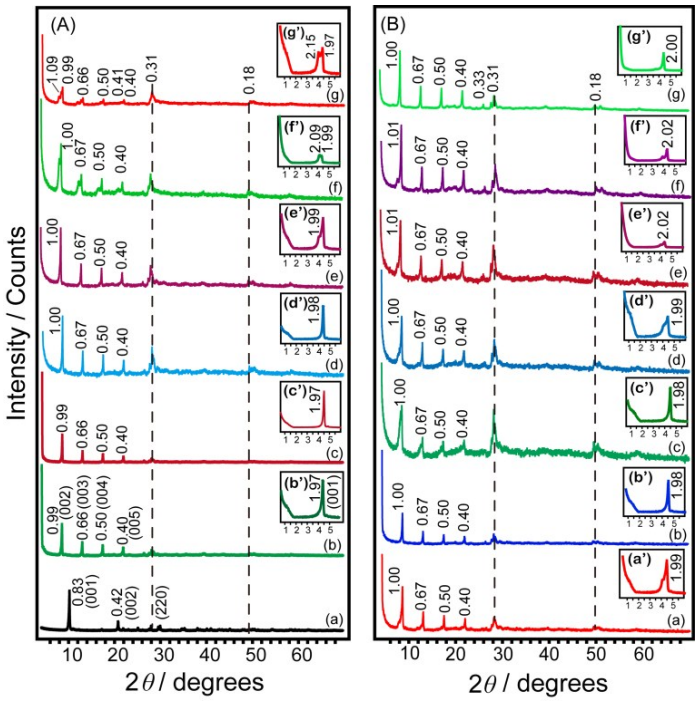

Fig. 1 (A) Powder XRD patterns of precursor Cl-LTbH (a), composites OS-LTbH (b, b') and OS_xCMA_{1-x}-LTbH: x = 0.9 (c, c'), 0.8 (d, d'), 0.7 (e, e'), 0.6 (f, f'), 0.5 (g, g'). (B) Powder XRD patterns of composites $CMA_{0.7}OS_{0.3}$-$LTb_yY_{1-y}H$: y = 1.0 (a, a'), 0.9 (b, b'), 0.7 (c, c'), 0.5 (d, d'), 0.3 (e, e'), 0.1 (f, f'), and 0 (g, g'). The *d*-values are given in nanometers.

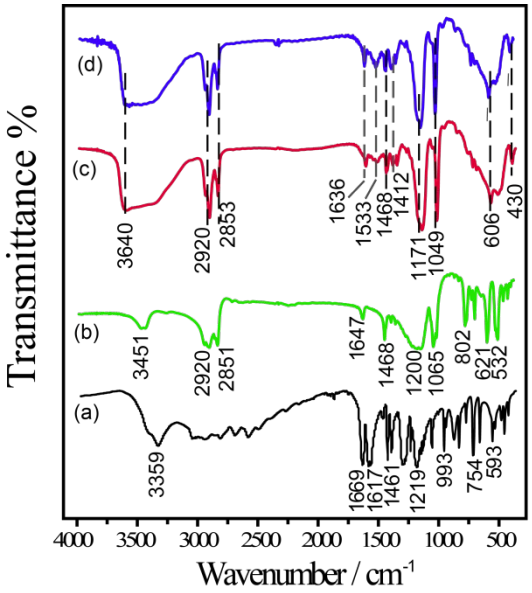

Fig. 2 FT-IR spectra of precursors CMA (a), OS (b), and composites OS_xCMA_{1-x}-LTbH: x = 0.6 (c) and 0.5 (d).

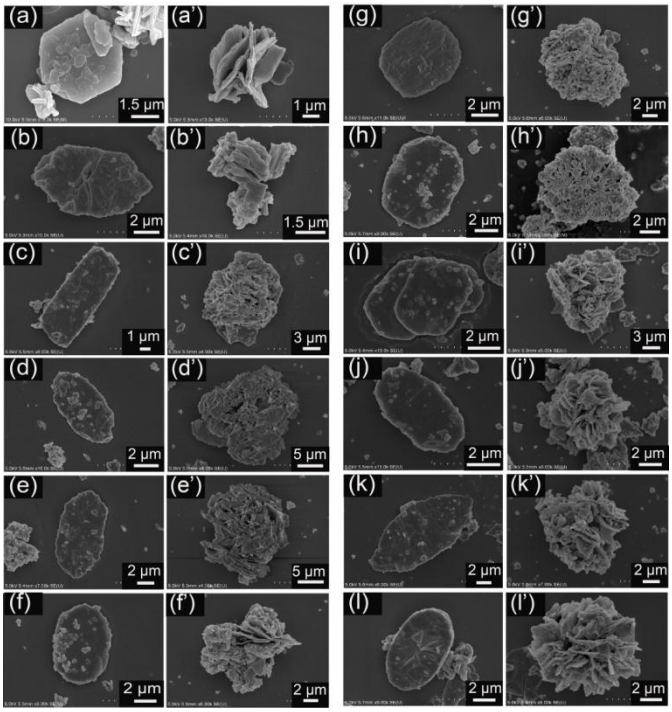

Fig. 3 SEM images of precursor Cl-LTbH (a, a'), OS_xCMA_{1-x}-LTbH composites: x = 0.9 (b, b'), 0.8 (c, c'), 0.7 (d, d'), 0.6 (e, e'), 0.5 (f, f'), and $CMA_{0.7}OS_{0.3}$-$LTb_yY_{1-y}H$ composites: y = 0.9 (g, g'), 0.7 (h, h'), 0.5 (i, i'), 0.3 (j, j'), 0.1 (k, k'), 0 (l, l').

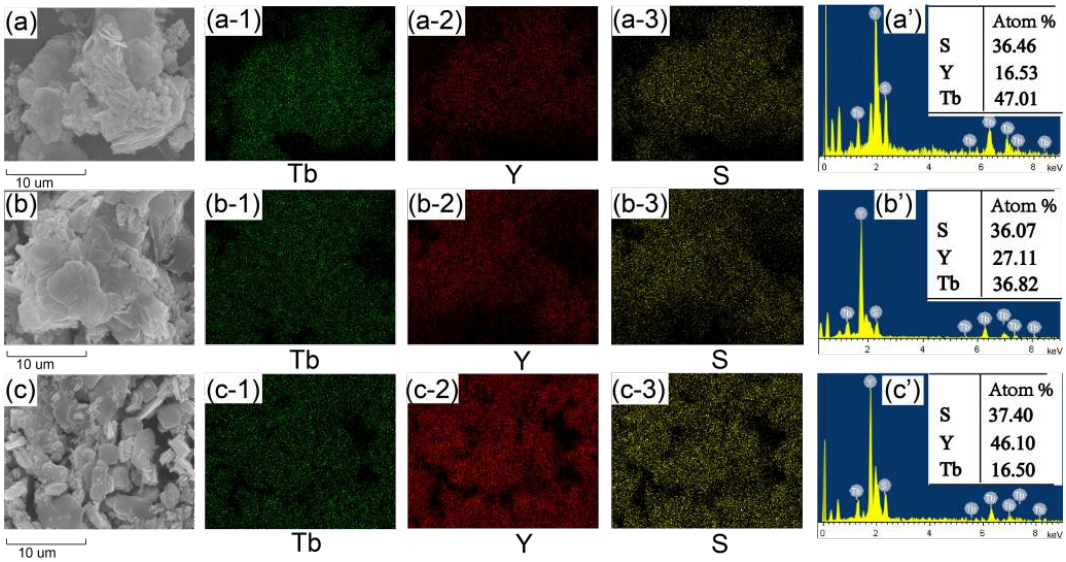

Fig. 4 SEM images of $CMA_{0.7}OS_{0.3}$-$LTb_yY_{1-y}H$: (a) y=0.7, (b) y=0.5, (c) y= 0.3; (a-1) to (a-3), (b-1) to (b-3) and (c-1) to (c-3) show corresponding elemental distribution maps of Tb, Y and S; a', b' and c' are related EDS and average compositions of a, b and c.

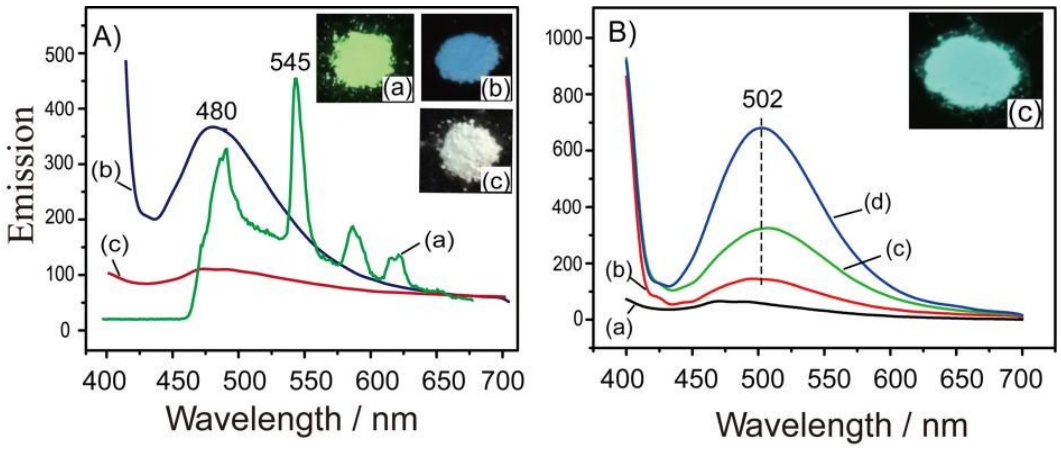

Fig. 5 (A) Powder emission spectra of precursors of Cl-LTbH (a), CMA-Na (b), and composite $OS_{0.9}CMA_{0.1}$-LTbH (c). The excitation wavelengths were 352 nm (a),420 nm (b) and 420 nm(c). (B) Powder emission spectra of $OS_{0.7}CMA_{0.3}$-$LTb_yY_{1-y}H$: y = 1 (a), y = 0.7 (b), y = 0.3 (c), y = 0 (d) . The excitation wavelengths were 420 nm for all of the samples. The insets are corresponding photographs under 365 nm UV irradiation.

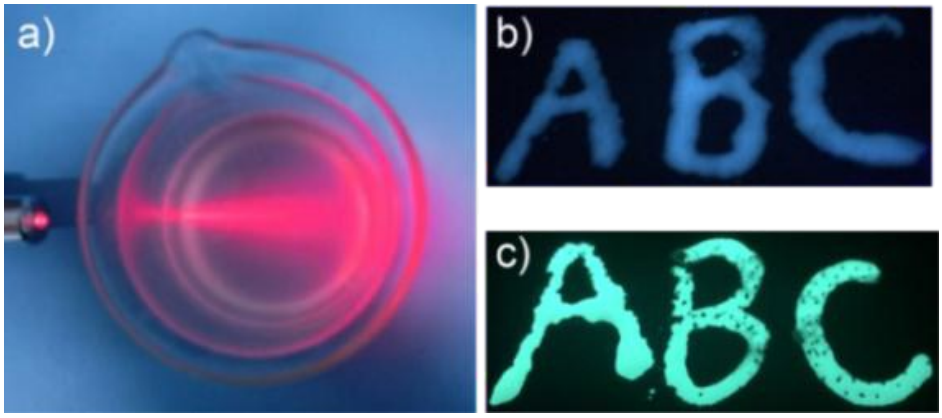

Fig. 6 (a) Tyndall light scattering of colloid suspensions of LRH composite in FM, and the ABC characters showing the (b) blue and green color (c) written by the colloidal suspensions of $CMA_{0.7}OS_{0.3}$-$LTb_{0.9}Y_{0.1}H$ and $CMA_{0.7}OS_{0.3}$-LYH, respectively.

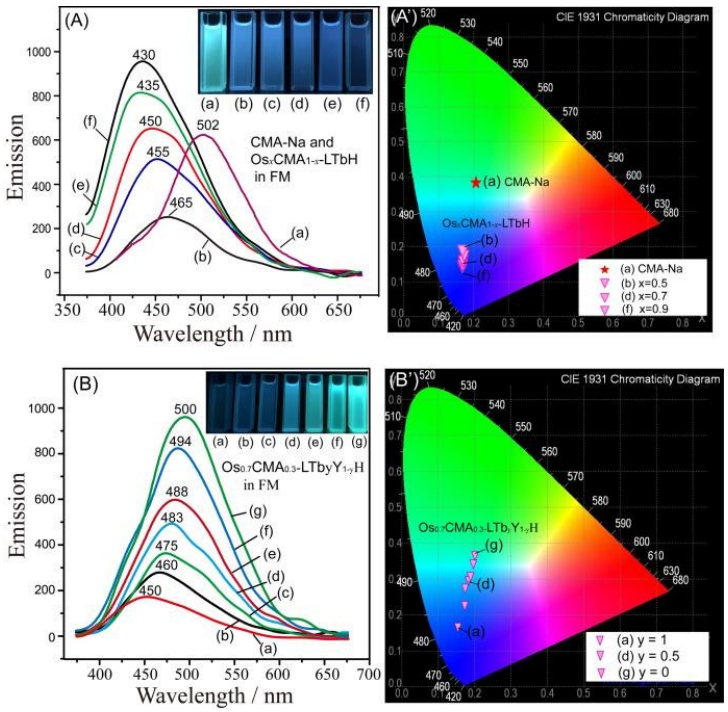

Fig. 7 (A) Emission spectra of CMA-Na (a) and OS_xCMA_{1-x}-LTbH composites in FM: x = 0.5 (b), 0.6 (c), 0.7 (d), 0.8 (e), 0.9 (f). The excitation wavelengths were 375 nm (a), 337 nm (b,c), 352 nm (d,e) and 355 nm (f). (B) Emission spectra of $CMA_{0.7}OS_{0.3}$-$LTb_yY_{1-y}H$ composites: y = 1.0 (a), 0.9 (b), 0.7 (c), 0.5 (d), 0.3 (e), 0.1 (f) and 0 (g) . The excitation wavelengths were 352 nm (a,b), 367 nm (c), 370 nm (d,e,f) and 375 nm (g). A′ and A′ are the CIE 1931 chromaticity diagrams of responding samples in (A) and (B) showing the photoluminescence color.

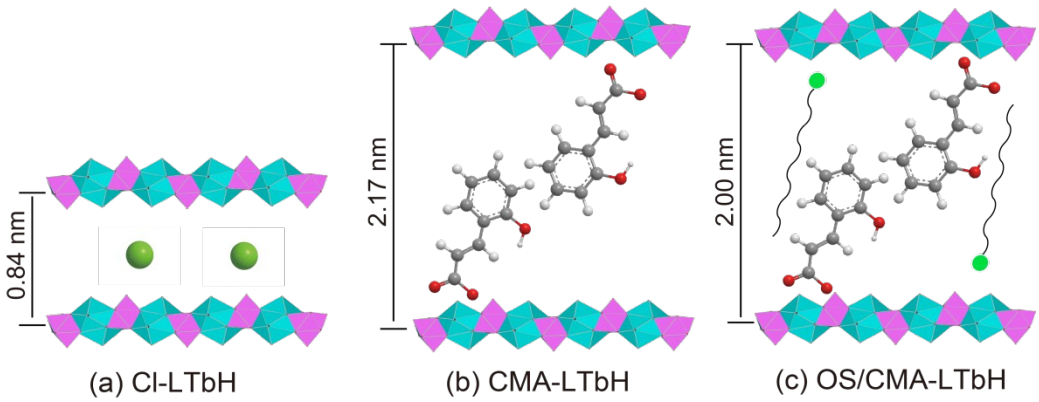

Scheme 1. Arrangements of gallery species in precursor Cl-LRH (a), and composites CMA-LRH (b), and OS/CMA-LRH (c), respectively.

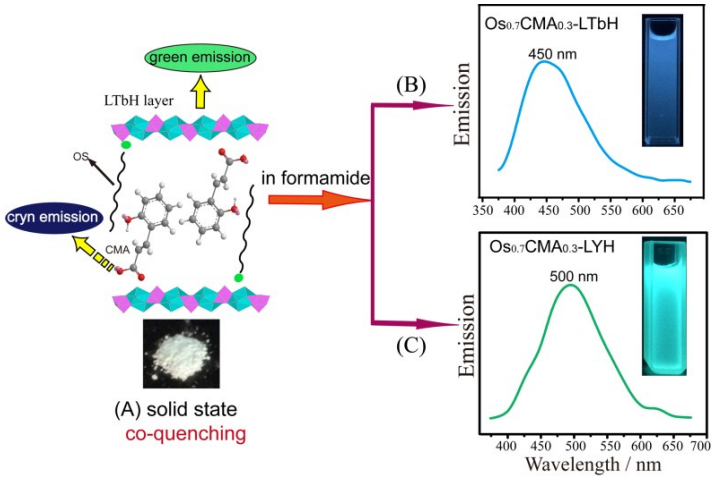

Scheme 2. OS/CMA-LRH composites showing versatile luminescence behaviors under different conditions: co-quencing in solid state (A), blue luminescence in formamide for delaminated LTbH layers (B), green luminescence in formamide for delaminated LYH layers (C).

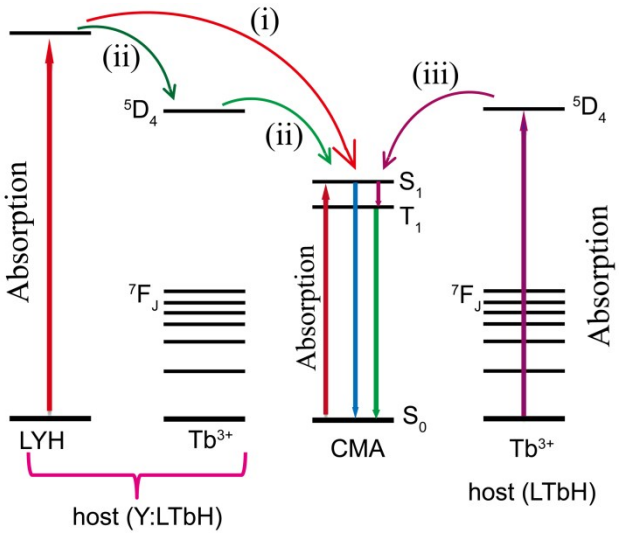

Scheme 3. Schematic representation of the energy transfer mechanism for composites OS/CMA-LRH.

Graphical Abstract

Delaminated Layered Rare-Earth Hydroxide Composites with Ortho-Coumaric Acid: Color-tunable luminescence and Blue Emission due to Energy Transfer

Feifei Su, Qingyang Gu, Shulan Ma,* Genban Sun, Xiaojing Yang, Li-Dong Zhao

LRH (R = Tb, Y) composites with ortho-coumaric acid and OS show color-tuing luminescence especially blue luminescence *via* energy transfer.